MAE 557 Mini-Project One

Yu Shuai

September 30, 2025

1 The 1D linear advection-diffusion problem

1.1 Two schemes for solving the equation

The equation we are going to solve is given as follows:

$$\frac{\partial u}{\partial t} + c\frac{\partial u}{\partial x} = \nu\frac{\partial^2 u}{\partial x^2}, \tag{1}$$

which is defined on the domain $x \in [0, 2\pi)$ with periodic boundary conditions. Assume we discretize the domain with a uniform spacing Δx to obtain a grid $\{x_i\}_{i=0}^{N_x-1}$ where

$$x_i = i\Delta x, \quad \Delta x = \frac{2\pi}{N_x}. \tag{2}$$

For the first scheme, we pick the forward Euler scheme for temporal discretization with timestep Δt:

$$\frac{\partial u(x,t)}{\partial t} \approx \frac{u(x,t+\Delta t) - u(x,t)}{\Delta t}, \tag{3}$$

and the first-order backward-biased upwind scheme for spatial discretization of the first derivative operator (without loss of generality, here we assume $c > 0$ to maintain the stability requirement for upwind scheme):

$$\frac{\partial u(x,t)}{\partial x} \approx \frac{u(x,t) - u(x-\Delta x,t)}{\Delta x}, \tag{4}$$

and the second-order centered scheme for the second derivative operator:

$$\frac{\partial^2 u(x,t)}{\partial x^2} \approx \frac{u(x+\Delta x,t) - 2u(x,t) + u(x-\Delta x,t)}{(\Delta x)^2}. \tag{5}$$

For the second scheme, we pick the backward Euler scheme for temporal discretization with timestep Δt:

$$\frac{\partial u(x,t)}{\partial t} \approx \frac{u(x,t) - u(x,t-\Delta t)}{\Delta t}, \tag{6}$$

and the second-order centered scheme for spatial discretization of the first derivative operator:

$$\frac{\partial u(x,t)}{\partial x} \approx \frac{u(x+\Delta x,t) - u(x-\Delta x,t)}{2\Delta x}, \tag{7}$$

and the second-order centered scheme for the second derivative operator:

$$\frac{\partial^2 u(x,t)}{\partial x^2} \approx \frac{u(x+\Delta x,t) - 2u(x,t) + u(x-\Delta x,t)}{(\Delta x)^2}. \tag{8}$$

1.1.1 Why second-order centered scheme for second-order spatial derivatives?

The reason why we should use a (second-order) centered scheme for the second derivative operator is that we don't want to introduce spurious propagation via the usage of non-centered second-order derivative scheme.

1.1.2 Write both semi-discrete governing equations in matrix form

Denote the semi-discrete solution $\boldsymbol{u}(t) \in \mathbb{R}^{N_x}$ as

$$\boldsymbol{u}(t) = \begin{bmatrix} u(x_0, t) \\ \vdots \\ u(x_{N_x-1}, t) \end{bmatrix} = \begin{bmatrix} u(0, t) \\ \vdots \\ u(2\pi - \Delta x, t) \end{bmatrix} \tag{9}$$

and the semi-discrete equation as

$$\frac{\mathrm{d}\boldsymbol{u}(t)}{\mathrm{d}t} = -\frac{c}{\Delta x}\mathbf{D}_1\boldsymbol{u}(t) + \frac{\nu}{(\Delta x)^2}\mathbf{D}_2\boldsymbol{u}(t). \tag{10}$$

In consideration of the periodic boundary conditions, for the first scheme, $\mathbf{D}_1$ is given as

$$\mathbf{D}_1 = \begin{bmatrix} 1 & 0 & \dots & 0 & -1 \\ -1 & 1 & \dots & 0 & 0 \\ \vdots & \vdots & \ddots & \vdots & \vdots \\ 0 & 0 & \dots & -1 & 1 \end{bmatrix}, \tag{11}$$

and $\mathbf{D}_2$ is given as

$$\mathbf{D}_2 = \begin{bmatrix} -2 & 1 & 0 & \dots & 1 \\ 1 & -2 & 1 & \dots & 0 \\ \vdots & \vdots & \ddots & \vdots & \vdots \\ 1 & 0 & \dots & 1 & -2 \end{bmatrix}. \tag{12}$$

For the second scheme, the matrix $\mathbf{D}_2$ is the same, but the matrix $\mathbf{D}_1$ now takes the form of

$$\mathbf{D}_1 = \begin{bmatrix} 0 & 1/2 & 0 & \dots & -1/2 \\ -1/2 & 0 & 1/2 & \dots & 0 \\ \vdots & \vdots & \ddots & \vdots & \vdots \\ 1/2 & 0 & \dots & -1/2 & 0 \end{bmatrix}. \tag{13}$$

1.2 Determine the theoretical stability limit

Since the domain is periodic, we can adopt the von Neumann stability analysis to investigate the stability limit. This is because for linear PDEs with periodic boundary conditions, the solutions can always be decomposed into linear combinations of Fourier modes. Suppose the solution takes the form of $u(x_j, t_n) = u(x_j, t_0)\sigma^n \exp(\mathrm{i}kx_j)$. For the first approach, we have

$$\frac{\partial u}{\partial t} + c\frac{\partial u}{\partial x} = \nu\frac{\partial^2 u}{\partial x^2} \tag{14a}$$

$$\Longrightarrow \frac{u(x, t+\Delta t) - u(x,t)}{\Delta t} = -c\frac{u(x,t) - u(x-\Delta x, t)}{\Delta x} + \nu\frac{u(x-\Delta x, t) - 2u(x,t) + u(x+\Delta x, t)}{(\Delta x)^2} \tag{14b}$$

$$\Longrightarrow \frac{\sigma - 1}{\Delta t} = -c\frac{1 - \exp(-\mathrm{i}\theta)}{\Delta x} + \nu\frac{\exp(\mathrm{i}\theta) - 2 + \exp(-\mathrm{i}\theta)}{(\Delta x)^2} \tag{14c}$$

$$\Longrightarrow \sigma = 1 - C(1 - \exp(-\mathrm{i}\theta)) + D(\exp(\mathrm{i}\theta) - 2 + \exp(-\mathrm{i}\theta)) \tag{14d}$$

$$\Longrightarrow \sigma = 1 - (C + 2D)(1 - \cos\theta) - \mathrm{i}C\sin\theta, \tag{14e}$$

where $C \overset{\text{def}}{=} c\Delta t/\Delta x$ is the CFL number, $D \overset{\text{def}}{=} \nu\Delta t/(\Delta x)^2$ is the diffusion number, and $\theta \overset{\text{def}}{=} k\Delta x$. For the stability limit, we need $|\sigma| \le 1$, which gives

$$\left|1 - (C + 2D)(1 - \cos\theta) - \mathrm{i}C\sin\theta\right| \le 1 \tag{15a}$$

$$\Longrightarrow (1 - (C + 2D)(1 - \cos\theta))^2 + C^2\sin^2\theta \le 1 \tag{15b}$$

$$\Longrightarrow -2(C + 2D)(1 - \cos\theta) + (C + 2D)^2(1 - \cos\theta)^2 + C^2\sin^2\theta \le 0 \tag{15c}$$

$$\Longrightarrow -2(1 + \frac{2}{Pe_{\Delta x}})(1 - \cos\theta) + C(1 + \frac{2}{Pe_{\Delta x}})^2(1 - \cos\theta)^2 + C(1 - \cos^2\theta) \le 0, \quad Pe_{\Delta x} \overset{\text{def}}{=} \frac{C}{D} \tag{15d}$$

$$\Longrightarrow -2(1 + \frac{2}{Pe_{\Delta x}}) + C(1 + \frac{2}{Pe_{\Delta x}})^2(1 - \cos\theta) + C(1 + \cos\theta) \le 0 \tag{15e}$$

$$\Longrightarrow C \le \frac{2(1 + \frac{2}{Pe_{\Delta x}})}{(1 + \frac{2}{Pe_{\Delta x}})^2(1 - \cos\theta) + (1 + \cos\theta)}. \tag{15f}$$

The inequality holds for any $\theta = k\Delta x > 0$, so we take $\theta = \pi$ and obtain the stability limit

$$C \leq \frac{1}{1 + \frac{2}{Pe_{\Delta x}}} = \frac{Pe_{\Delta x}}{Pe_{\Delta x} + 2}, \qquad D = \frac{C}{Pe_{\Delta x}} \leq \frac{1}{Pe_{\Delta x} + 2}. \Longrightarrow \Delta t \leq \frac{(\Delta x)^2}{2\nu + c\Delta x} \tag{16}$$

At $(c, \nu) = (1, 0.01)$, we have

$$\Delta t \leq \frac{(\Delta x)^2}{0.02 + \Delta x}, \tag{17}$$

and at $(c, \nu) = (1, 1)$, we have

$$\Delta t \leq \frac{(\Delta x)^2}{2 + \Delta x}. \tag{18}$$

Similarly, for the second approach, we have

$$\frac{\partial u}{\partial t} + c\frac{\partial u}{\partial x} = \nu\frac{\partial^2 u}{\partial x^2} \tag{19a}$$

$$\Longrightarrow \frac{u(x,t) - u(x,t-\Delta t)}{\Delta t} = -c\frac{u(x+\Delta x,t) - u(x-\Delta x,t)}{2\Delta x} + \nu\frac{u(x-\Delta x,t) - 2u(x,t) + u(x+\Delta x,t)}{(\Delta x)^2} \tag{19b}$$

$$\Longrightarrow \frac{1-\sigma^{-1}}{\Delta t} = -c\frac{\exp(\mathrm{i}\theta) - \exp(-\mathrm{i}\theta)}{2\Delta x} + \nu\frac{\exp(\mathrm{i}\theta) - 2 + \exp(-\mathrm{i}\theta)}{(\Delta x)^2} \tag{19c}$$

$$\Longrightarrow \sigma^{-1} = 1 + \mathrm{i}C\sin\theta + 4D\sin^2(\theta/2), \tag{19d}$$

which indicates that $|\sigma| \leq 1$ for all C, D and θ and that the second approach is unconditionally stable.

1.3 Determine the conservation properties at $\nu = 0$

1.3.1 Why we need to investigate the problem at $\nu = 0$?

The reason is because if we want to study whether our numerical schemes preserve the secondary conservation property, i.e. energy conservation, then we must pick a governing equation that inherently possess this conservation property. At $\nu > 0$, the equation has a positive diffusion term and thus the energy will dissipate over time.

1.3.2 The primary conservation property

The primary conservation property requires that the integral

$$\int_0^{2\pi} u(x,t)\mathrm{d}x \tag{20}$$

does not change over timesteps. Notice that this integral is proportional to the amplitude of the zero-frequency Fourier component. Thus, if we utilize the solution form $u(x_j, t_n) = u(x_j, t_0)\sigma^n \exp(\mathrm{i}kx_j)$, then we only need $\sigma = 1$ when $k = 0$, i.e. when $\theta = k\Delta x = 0$. Examining (14) and (19), we find that both schemes satisfy this requirement. Therefore, both approaches preserve the primary conservation property.

1.3.3 The secondary conservation property

The secondary conservation property requires that the integral

$$\int_0^{2\pi} |u|^2(x,t)\mathrm{d}x \tag{21}$$

does not change over timesteps. Again, if we utilize the solution form $u(x_j, t_n) = u(x_j, t_0)\sigma^n \exp(\mathrm{i}kx_j)$, then this requires that $|\sigma| \equiv 1$ for all k. For the first approach, we have $\sigma = 1 - C(1 - \cos\theta) - \mathrm{i}C\sin\theta$ from (14) at $\nu = 0$. Then

$$\begin{aligned} |\sigma|^2 &= 1 - 2C(1-\cos\theta) + C^2(1-\cos\theta)^2 + C^2\sin^2\theta \\ &= 1 + 2C(C-1)(1-\cos\theta), \end{aligned} \tag{22}$$

which means that when $C = 1$ or $c\Delta t = \Delta x$, the first approach is energy-conserving. Otherwise, it is not energy-conserving.

For the second approach, we have $\sigma^{-1} = 1 + \mathrm{i}C\sin\theta$ from (19) at $\nu = 0$. Since $C > 0$, the second approach is unconditionally not energy conserving.

1.3.4 Effects on solutions with non-conserving schemes

When $C > 0$, the second approach does not satisfy the secondary conservation. Since $\sigma^{-1} = 1 + \mathrm{i}C\sin\theta$, we always have $|\sigma| < 1$ indicating that the solution will decay at long time. To diminish the numerical dissipation, a feasible way is to decrease $C = c\Delta t/\Delta x$, which requires us to decrease the timestep Δt or increase the spacing Δx while keeping $(\Delta t, \Delta x)$ is still within the stability limit.

For the first approach, since $|\sigma|^2 = 1 + 2C(C-1)(1-\cos\theta)$, the total energy of solution will increase over time when $C > 1$, which means that the solution will become unstable eventually. This is consistent with our previous study on the stability limit $C \le Pe_{\Delta x}/(Pe_{\Delta x} + 2)$ (which gives $C \le 1$ at $\nu = 0$). Conversely, the energy will decrease when $C < 1$. To mitigate this degradation, a possible way is to increase C making it as close to 1 as possible.

1.3.5 Effects on solutions with conserving schemes

From the above analysis, we know that when $C = 1$ and $\nu = 0$, our first approach does satisfy both conservation properties. However, there is a trade-off that we need to fix $\Delta x = c\Delta t$. If Δt is small, then one need to use many spatial points to form a fine grid. Additionally, keeping C at the stability margin is often not a good choice since any numerical inaccuracy will breach this stability limit and set the numerical solution unstable.

1.3.6 Properties of discretization to maintain secondary conservation

Generally speaking, spatial discretization and temporal advancing schemes have to be "centered" to maintain secondary conservation. For example, we may use centered schemes to discretize differential operators, and the trapezoid method for temporal discretization.

2 The Burgers equation

2.1 How the nonlinearity affects the convergence and stability characteristics

For the convergence characteristics, we know that our first approach has first-order accuracy in time (Forward Euler) and first-order accuracy (first-order upwind scheme for first-order derivative) in space, and that our second approach has first-order accuracy in time (Forward Euler) and second-order accuracy (centered scheme) in space. However, recall that the Burgers' equation will exhibit spatial discontinuity in its solutions. Therefore, all our convergence results (or accuracy) that are based on the assumption of smooth functions will fail to reflect the actual characteristics of our schemes. In this case, the orders of discretization errors tend to be $O(1)$. Nevertheless, if the solutions are still globally smooth in space and time (at least in a small timespan before the shock wave emerges), then the convergence characteristics (i.e. the accuracy) should be the same as the linear case.

For the (nonlinear) stability characteristics, we cannot adopt the von Neumann analysis directly. Nevertheless, a heuristic approach is to replace the constant advection speed c with the actual velocity u. For the first numerical approach, the stability for linear equation gives $\Delta t \le (\Delta x)^2/(2\nu + c\Delta x)$, so qualitatively the stability for Burgers' equation should take the form of $\Delta t \le (\Delta x)^2/(2\nu + \max_t[\|u\|(t)]\Delta x)$, where $\|u\|(t)$ should be defined as the maximal absolute value of $u(x,t)$ for all x at a given time t:

$$\|u\|(t) \overset{\text{def}}{=} \max_x |u(x,t)|. \tag{23}$$

Given that our initial condition is $u(x,0) = \sin(x)\exp(-(x-\pi)^2)$ and that the Burgers' equation is a parabolic PDE, we have $\max_t[\|u\|(t)] = \|u\|(0) \approx 0.4$. Consequently, we can expect that a sufficient condition for stability of the first numerical approach is

$$\Delta t \le \frac{(\Delta x)^2}{2\nu + \max_t[\|u\|(t)]\Delta x} = \frac{(\Delta x)^2}{2\nu + 0.4\Delta x}, \tag{24}$$

which actually relaxes the restriction of Δt compared to the linear advection-diffusion equation with $c = 1$.

For the second numerical approach, since we have already shown that it is unconditionally stable regardless of the CFL number and the diffusion number. Based on our heuristic analysis, we believe that it should be still numerically stable when applied to the Burgers' equation.

2.2 Numerical solutions and convergence analysis

2.2.1 The explicit approach

To study the spatial convergence of our explicit numerical approach, we fix $\Delta t = 0.001$ and set the number of grid points to be $N_x = 10, 20, 30, 40, 60$ with the spacing $\Delta x = L/N_x$. The error is evaluated as the pointwise difference between the numerical solutions and a high-fidelity solution $\tilde{u}$ solved with $N_x = 120$ on each grid point at $(x,t) = (L/5, 1)$:

$$\epsilon = |u(L/5,1) - \tilde{u}(L/5,1)|. \tag{25}$$

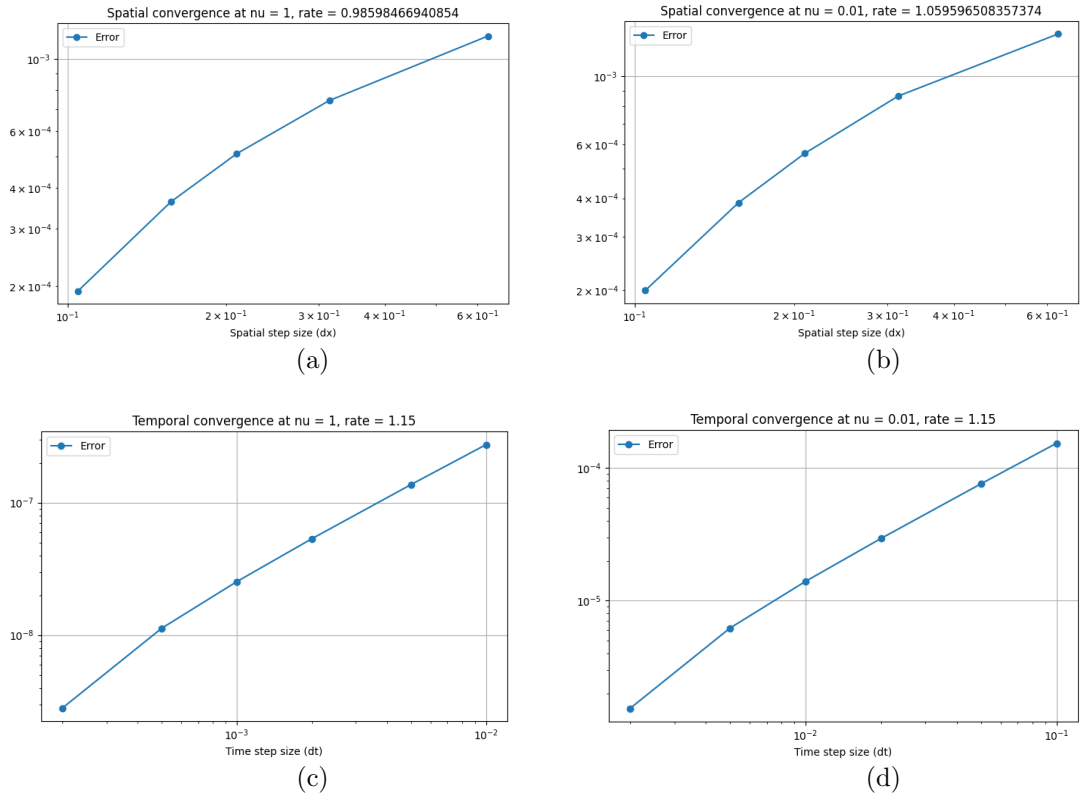

Figure 1: Panel (a)-(b): spatial convergence of the explicit approach at $\nu = 1$ and $\nu = 0.01$ respectively. Panel (c)-(d): temporal convergence of the explicit approach at $\nu = 1$ and $\nu = 0.01$ respectively.

Fig. 1(a)-(b) shows the convergence of our spatial discretization schemes at $\nu = 1$ and $\nu = 0.01$, respectively. The results show that the rate of convergence is $O(\Delta x)$, which is consistent with the discretization accuracy of the right-hand side of Burgers' equation determined by the first-order upwind scheme for the discretization of the advection term.

Similarly, we study the temporal convergence via fixing $N_x = 40$ and setting $\Delta t = 0.01, 0.005, 0.002, 0.001, 0.0005, 0.0002$. The error is evaluated as the root-mean-square of difference between the numerical solutions and a high-fidelity solution $\tilde{u}$ solved with $\Delta t = 0.0001$ on each grid point at final time $t = T = 10$:

$$\epsilon = \frac{1}{N_x} \sum_{i=0}^{N_x - 1} |u(x_i, T) - \tilde{u}(x_i, T)|^2, \quad x_i = \frac{i}{N_x} L. \tag{26}$$

Fig. 1(c)-(d) shows the convergence of our forward-Euler temporal discretization at $\nu = 1$ and $\nu = 0.01$, respectively. At both parameters, the rate of convergence is $O(\Delta t)$, which is consistent with the accuracy of forward-Euler scheme.

For the stability characteristics, we find that the nonlinearity of Burgers' equation allows us to pick a timestep Δt slightly larger than the theoretical prediction (24). For instance, at $\nu = 1$ and $N_x = 40$, the maximal allowable timestep according to (24) is $\Delta t \approx 0.0119$, while at $\nu = 0.01$ it is 0.30012. However, Fig. 2 shows that at $\nu = 1$, the maximal allowable timestep should be between 0.012 and 0.013, and at $\nu = 0.01$ the maximal allowable timestep is between 0.9 and 1.

2.2.2 The implicit approach

To study the spatial convergence of our implicit numerical approach, we fix $\Delta t = 0.001$ and set the number of grid points to be $N_x = 10, 20, 30, 40, 60$ with the spacing $\Delta x = L/N_x$. A newton method is adopted to solve the nonlinear equation at each timestep with a 10^{-12} residual threshold. The error is evaluated as the pointwise difference between the numerical solutions and a high-fidelity solution $\tilde{u}$ solved with $N_x = 120$ on each grid point at $(x, t) = (L/5, 1)$:

$$\epsilon = |u(L/5, 1) - \tilde{u}(L/5, 1)|. \tag{27}$$

Fig. 3(a)-(b) shows the convergence of our spatial discretization schemes at $\nu = 1$ and $\nu = 0.01$, respectively. The results show that the rate of convergence is $O((\Delta x)^2)$, which is consistent with the discretization accuracy of the second-order central scheme for both the advection and the diffusion terms.

Similarly, we study the temporal convergence via fixing $N_x = 40$ and setting $\Delta t = 0.1, 0.05, 0.02, 0.01$. The error is evaluated as the root-mean-square of difference between the numerical solutions and a high-fidelity solution $\tilde{u}$ solved with

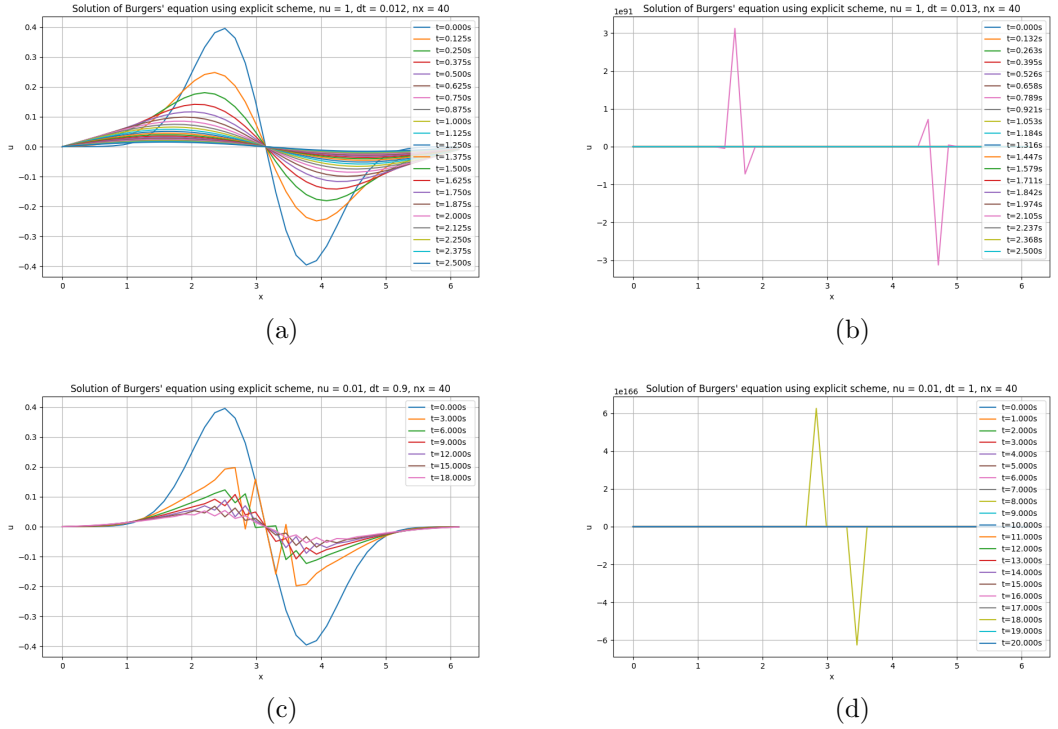

Figure 2: Solutions of Burgers' equation at different ν and Δt using the explicit approach for stability analysis.

$\Delta t = 0.001$ on each grid point at final time $t = T = 10$:

$$\epsilon = \frac{1}{N_x} \sum_{i=0}^{N_x - 1} |u(x_i, T) - \tilde{u}(x_i, T)|^2, \quad x_i = \frac{i}{N_x} L. \tag{28}$$

Fig. 3(c)-(d) shows the convergence of our backward-Euler temporal discretization at $nu = 1$ and $nu = 0.01$, respectively. At both parameters, the rate of convergence is $O(\Delta t)$, which is consistent with the accuracy of backward-Euler scheme.

For the stability characteristics, we find that the implementation of the implicit numerical approach does enable us to pick a very large timestep even with a small Δx. As shown in Fig. 4, we can obtain solutions with good fidelity on a fine grid $N_x = 120$ but with a large timestep $\Delta t = 1$, which validates our theoretical analysis that the usage of implicit timesteppers greatly increase the maximal limit of timestep.

2.3 Conservation properties at $\nu = 0$

At $\nu = 0$, the first approach gives the discretized equation in the form of

$$u_j^{n+1} = u_j^n + \frac{\Delta t}{\Delta x} \left(\frac{u_j^n + |u_j^n|}{2} (u_j^n - u_{j-1}^n) + \frac{u_j^n - |u_j^n|}{2} (u_{j+1}^n - u_j^n) \right). \tag{29}$$

To check the primary conservation property, we sum both sides of (29) across the spatial domain:

$$\begin{aligned} \sum_j u_j^{n+1} &= \sum_j u_j^n + \frac{\Delta t}{\Delta x} \sum_j \left(\frac{u_j^n + |u_j^n|}{2} (u_j^n - u_{j-1}^n) \right) + \frac{\Delta t}{\Delta x} \sum_j \left(\frac{u_j^n - |u_j^n|}{2} (u_{j+1}^n - u_j^n) \right) \\ &= \sum_j u_j^n - \frac{\Delta t}{2\Delta x} \sum_j (|u_j^n| (u_{j-1}^n - 2u_j^n + u_{j+1}^n)) \\ &\neq \sum_j u_j^n, \end{aligned} \tag{30}$$

which indicates that this approach does not preserve the primary conservation. Similar checks can be performed to conclude that the approach does not preserve the secondary conservation either. To validate our theoretical analysis, we plot the primary and secondary conservative quantity with time in Fig. 5(a) and (b) indicating their time evolution. This is in contrast to the case of the linear advection-diffusion equation where our first approach does satisfy the primary conservation property. The difference is due to the fact that Burgers' equation has a locally velocity-dependent advection

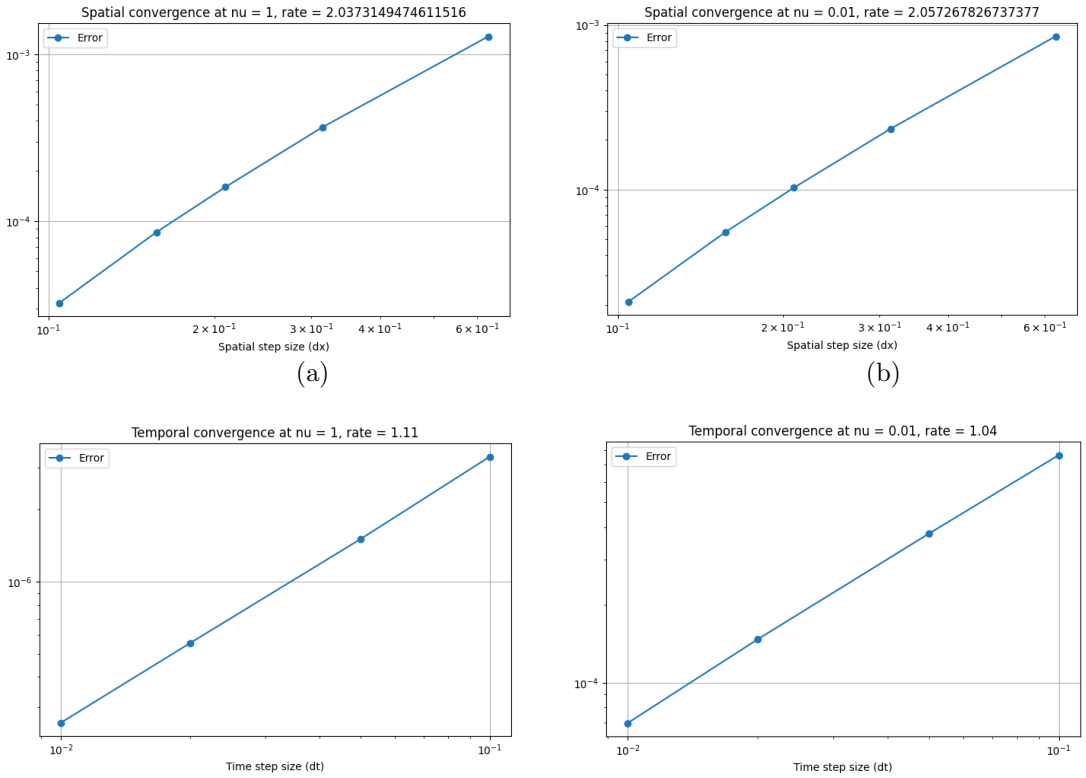

Figure 3: Panel (a)-(b): spatial convergence of the implicit approach at $\nu = 1$ and $\nu = 0.01$ respectively. Panel (c)-(d): temporal convergence of the implicit approach at $\nu = 1$ and $\nu = 0.01$ respectively.

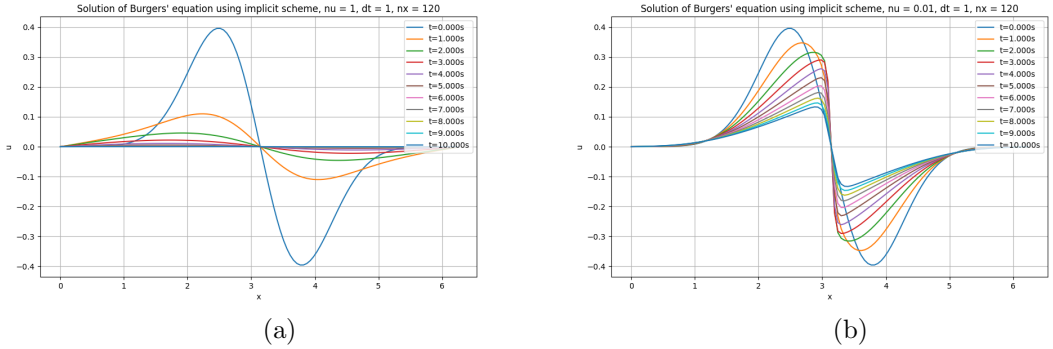

Figure 4: Solutions of Burgers' equation at different ν and Δt using the implicit approach for stability analysis.

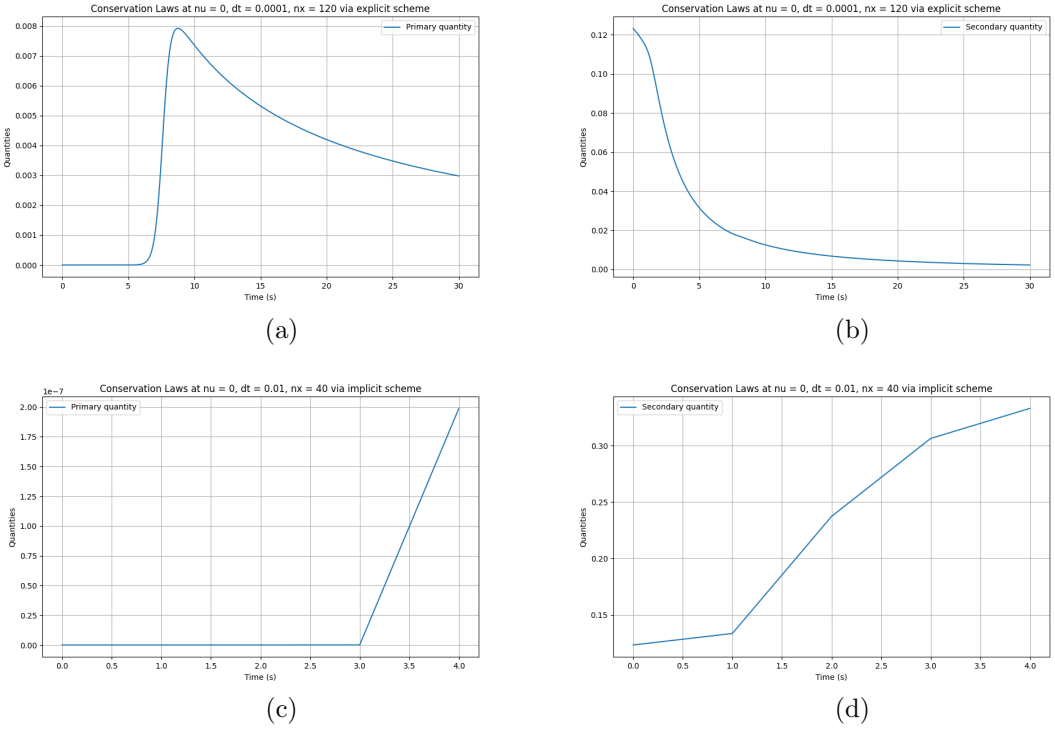

Figure 5: Time evolution of primary and secondary conservative quantities $\sum_j u_j$ and $\sum_j |u_j|^2$ computed from the solutions solved via both approaches.

speed that decides the bias direction of the upwind scheme. Therefore, the discretized nonlinearity cannot be written in a uniform flux form, and the numerical solution will have time-varying u summed across the domain.

On the other hand, the second approach gives the discretized equation in the form of

$$u_j^{n+1} = u_j^n + \frac{\Delta t}{2\Delta x} u_j^{n+1}(u_{j+1}^{n+1} - u_{j-1}^{n+1}), \tag{31}$$

which turns out to preserve the primary conservation property since

$$\begin{aligned}
\sum_j u_j^{n+1} &= \sum_j u_j^n + \frac{\Delta t}{2\Delta x} \sum_j (u_j^{n+1} u_{j+1}^{n+1} - u_j^{n+1} u_{j-1}^{n+1}) \\
&= \sum_j u_j^n + \frac{\Delta t}{2\Delta x} \sum_{j=0}^{N_x - 1} u_j^{n+1} u_{j+1}^{n+1} - \frac{\Delta t}{2\Delta x} \sum_{j=-1}^{N_x - 2} u_j^{n+1} u_{j+1}^{n+1} \\
&= \sum_j u_j^n
\end{aligned} \tag{32}$$

under the periodic boundary conditions. Nevertheless, the secondary conservation property is violated since

$$\begin{aligned}
\sum_j (u_j^{n+1})^2 &= \sum_j (u_j^n + \frac{\Delta t}{2\Delta x}(u_j^{n+1} u_{j+1}^{n+1} - u_j^{n+1} u_{j-1}^{n+1}))^2 \\
&= \sum_j \left((u_j^n)^2 + \frac{\Delta t}{\Delta x} u_j^n (u_j^{n+1} u_{j+1}^{n+1} - u_{j-1}^{n+1} u_j^{n+1}) + \frac{(\Delta t)^2}{4(\Delta x)^2} ((u_j^{n+1} u_{j+1}^{n+1})^2 - 2 u_j^{n+1} u_{j+1}^{n+1} u_j^{n+1} u_{j-1}^{n+1} + (u_j^{n+1} u_{j-1}^{n+1})^2) \right) \\
&\neq \sum_j u_j^n.
\end{aligned} \tag{33}$$

To validate our theoretical analysis, we plot the primary and secondary conservative quantity with time in Fig. 5(c) and (d) indicating their time evolution. If we ignore the numerical artefacts in the time evolution of primary conservative quantity, then we can conclude that the second approach preserves the primary conservation while violates the secondary conservation.

To ensure the primary conservation, we should reformulate the Burgers' equation at $\nu = 0$ in the form as follows:

$$\frac{\partial u}{\partial t} + u \frac{\partial u}{\partial x} = 0 \Longrightarrow \frac{\partial u}{\partial t} + \frac{\partial (u^2/2)}{\partial x} = 0, \tag{34}$$

such that

$$\int_0^L (\frac{\partial u}{\partial t} + \frac{\partial (u^2/2)}{\partial x}) \mathrm{d}x = 0$$
$$\Longrightarrow \frac{\mathrm{d}}{\mathrm{d}t} \int_0^L u(x,t) \mathrm{d}x = \frac{u^2(x,t)}{2}\Big|_{x=0}^{x=L} \equiv 0 \tag{35}$$

Additionally, to ensure the secondary conservation, we should reformulate the Burgers' equation at $\nu = 0$ in the form as follows:

$$\frac{\partial u}{\partial t} + u\frac{\partial u}{\partial x} = 0 \Longrightarrow u\frac{\partial u}{\partial t} + u^2\frac{\partial u}{\partial x} = 0 \Longrightarrow \frac{\partial (u^2/2)}{\partial t} + \frac{\partial (u^3/3)}{\partial x} = 0. \tag{36}$$

2.4 Long-time solutions at $\nu = 0.01$

At $\nu = 0.01$, the Burgers' equation has a very small viscosity, which allows the formation of shocks at long time causing numerical challenges. In this case, second-order central scheme applied to the advection term in our second approach will introduce spurious oscillations since it does not introduce numerical dissipation and thus has large overshoots near the shock fronts. To eliminate the oscillations, one can switch to the first-order upwind scheme for discretization of the advection term. However, we are now sacrificing the accuracy of spatial discretization by replacing a second-order scheme with a first-order scheme.

2.5 Summary: pros and cons of explicit schemes vs implicit schemes

From our analysis and implementation of both numerical approaches shown above, we find that the explicit scheme has the following pros and cons:

- 1. simple and intuitive, very easy to implement in coding;
- 2. straightforward and cheap in timestepping, no need to solve nonlinear equations at each timestep;
- 3. easy to analyze stability and conservation properties theoretically;
- 4. strict stability constraints, need to carefully choose timestep and grid spacing resulting in a potentially long runtimes.

Conversely, the implicit scheme has the following pros and cons:

- 1. Good stability for long-term simulation;
- 2. Not straightforward and expensive in implementation, need to solve nonlinear equations at each timestep;
- 3. Not easy to analyze conservation properties theoretically;
- 4. Picking a large timestep is allowable but may sacrifice the accuracy

...

References